

Las Matras Block, Central Argentina (37°S–67°W): the Southernmost Cuyania Terrane and its Relationship with the Famatinian Orogeny

Ana María Sato^{1*}, Hugo Tickyj², Eduardo Jorge Llambías¹, Miguel Angelo Stipp Basei³ and Pablo Diego González¹

¹ Centro de Investigaciones Geológicas, CONICET-Universidad Nacional de La Plata, Calle 1 N° 644, B1900TAC La Plata, Argentina, E-mail: sato@cig.museo.unlp.edu.ar; llambias@cig.museo.unlp.edu.ar; gonzapab@cig.museo.unlp.edu.ar

² Universidad Nacional de La Pampa. Av. Uruguay 151, L6300CLB Santa Rosa, La Pampa, Argentina, E-mail: htickyj@exactas.unlpam.edu.ar

³ CPGeo, Instituto de Geociências, Universidade de São Paulo, São Paulo SP 05422-970, Brazil, E-mail: baseimas@usp.br

* Corresponding author

(Manuscript received August 15, 2003; accepted February 9, 2004)



Abstract

The Las Matras Block in Central Argentina constitutes the southernmost part of the Cuyania terrane, which was accreted to the southwestern margin of Gondwana during the Early to Mid Ordovician Famatinian orogeny. The Grenville-aged rocks of the Las Matras Block are represented by the tonalitic to trondhjemitic Las Matras pluton. A new U-Pb conventional zircon age of 1244 ± 42 Ma confirms previous Sm-Nd and Rb-Sr isochron ages of this pluton. Mineral composition data are consistent with the tonalitic-trondhjemitic character of the pluton, and constrain its emplacement level to 1.9 to 2.6 kb. This shallow level of emplacement and the undeformed character of the pluton are distinctive features of this southernmost basement. A regional comparison indicates that the igneous-metamorphic evolution of the Grenville-aged basement rocks of the Cuyania terrane occurred over a period of more than 200 million years, with ages older than 1200 Ma up to those close to 1000 Ma. The shallowest crustal level is found in Las Matras, suggesting a southward shallowing of the exposed level of basement. The deformation and metamorphism associated with the collisional Famatinian orogeny affect both the Cuyania terrane and the adjacent western margin of Gondwana, and the Gondwana margin was also the locus of the related arc magmatism, but the compressive effects of the collision decrease in intensity toward the south. The Famatinian metamorphism and magmatism continue even further south into the Patagonia region, but the southern continuity of the Cuyania terrane into this region remains uncertain.

Key words: Cuyania terrane, Grenville orogeny, Famatinian orogeny, trondhjemitic, Gondwana.

Introduction

The Early Paleozoic geological history of central and northwestern Argentina is characterized by an interaction between an allochthonous composite terrane showing Laurentian affinities (the Cuyania terrane, Ramos, 1995; Ramos et al., 1998) and the southwestern margin of Gondwana, where the earlier Neoproterozoic to Cambrian “Pampean” orogenic cycle had developed (Fig. 1). An extensive Ordovician magmatic arc occurred along the Gondwana margin (mainly Eastern Sierras Pampeanas, *sensu* Caminos, 1979) prior to the accretion of Cuyania in the Early to Middle Ordovician. The penetrative deformation and regional low- to high-grade metamorphism associated

with the collision overprinted both the Gondwana margin and the Cuyania terrane, which as a whole make up the so-called Famatinian orogen (Famatinian cycle, Aceñolaza and Toselli, 1976).

The southernmost outcrops belonging to the Cuyania terrane are found in the Las Matras Block (around 37°S), which is located close to the corresponding southernmost exposures of the Eastern Sierras Pampeanas, in the Chadileuvú Block (Fig. 1). Together these blocks constitute the southern part of the Famatinian orogen, and therefore provide an opportunity to identify any N-S variability in Famatinian orogenic conditions.

In this contribution, we report new information on the age and petrographic features of the Grenville-aged Las

Matras pluton, including electron probe microanalytical data (EPMA) on minerals and one conventional U-Pb zircon age. This new information adds to the general characterization and interpretation given in Sato et al. (2000), especially in constraining age and the emplacement depth. Additionally, the discussion below emphasizes a comparison of the Las Matras pluton with the rest of the Grenvillian basement in the Cuyania terrane, and the relationship of this terrane with the autochthonous Gondwanian Chadileuvú Block within the context of the Famatinian orogen.

The Las Matras Block

The Las Matras Block was named by Sato et al. (2000) in order to distinguish the pre-Permian geology of the northwestern part of the La Pampa Province (Linares et al., 1980; Tickyj, 1999) from that of the Chadileuvú Block in the southeastern part. The Las Matras Block is characterized mainly by Grenville-aged plutonic rocks and a Cambro-Ordovician sedimentary cover (see main features in Fig. 2), typical of the rock associations found elsewhere in the Cuyania terrane, such as to the north in the San Rafael Block and in the Pie de Palo, Precordillera, and Umango areas.

Although the Las Matras basement is exposed over an area of only 4 km by 4 km, the geophysical information of Chernicoff and Zappettini (2003) suggests a wider subsurface extension, with the possibility of a connection to the garnetiferous schists located about 70 km to the north of Las Matras (Well IV-D; Criado Roqué, 1979). It is also possible that the rocks of the Las Matras Block underlie a considerable region extending to the northwest, to the few outcrops of micaschists and migmatites of the Cerro Las Pacas Formation (Holmberg, 1973) located to the northwest of Las Matras at around 35°45'S – 68°45'W, and even up to the Grenvillian Cerro La Ventana Formation of the San Rafael Block (Criado Roqué, 1972; Cingolani and Varela, 1999).

Within the sedimentary cover, the well studied carbonate platform deposits of San Jorge Formation (Melchor et al., 1999a,b; Tickyj et al., 2002) form small and scattered outcrops aligned to a NW trend, (between 36°49'38"S/67°19'19"W and 37°28'49"S/66°25'25"W, within the Las Matras Block). The San Jorge Formation is considered to represent the southernmost exposure of the Early Paleozoic carbonate platform of the Precordillera (Astini et al., 1995; Melchor et al., 1999c; Tickyj et al., 2002). However, the significance of occurrences of similar limestones to the southeast in the area of Chadileuvú Block is unclear. These limestones are in close spatial association with quartz arenites previously assigned to the Carboniferous Agua Escondida Formation. According to

Melchor et al. (1999c), those quartz arenites found in close association with the San Jorge Formation and exhibiting evidence of a stronger deformation style probably belong to the Cambro-Ordovician platform deposits, and should be separated from the much younger Agua Escondida Formation.

Grenvillian Las Matras Pluton

The single exposure of this pluton is located in the northwestern La Pampa Province (36°46'S/67°07'W). Modern sediments cover the area, and contacts with country rock were not observed. The internal facies are

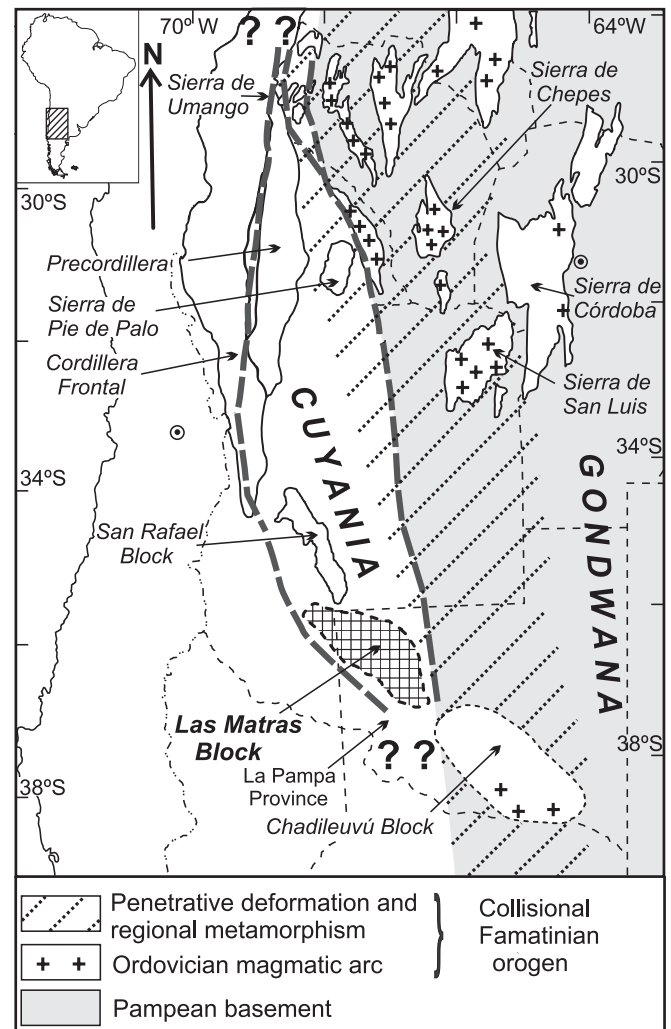


Fig. 1. Early Paleozoic tectonic relationship between the proto-Andean Gondwana margin and the accreted Cuyania terrane. The Pampean basement of Gondwana margin is intruded by the extensive Ordovician magmatic arc. The compressive deformation and regional metamorphism associated with the collision overprint both the Cuyania terrane and the Gondwana border. Within the resultant Famatinian orogen, the compressive regime decreases from north to south, and from the suture zone toward the east.

defined on the basis of proportions of tonalitic enclaves contained in the trondhjemitic host rocks. The most abundant facies are trondhjemitic, and they contain variable proportions of tonalitic enclaves with globular and irregular shapes and rounded to angular contours. Some minor areas are more homogeneously tonalitic. Occasional thin dykes of varied composition and random orientation cut the pluton.

A distinctive feature of this pluton is its undeformed character. The original enclave shapes and the magmatic texture and mineralogy of the tonalites and trondhjemitites being well preserved (see field pictures and photomicrographs in Sato et al., 2000). On geochemical and isotopic basis, the tonalitic and trondhjemitic facies have a cogenetic origin.

Petrography and EPMA mineral data

Tonalites are dark gray, fine-grained equigranular rocks. Modal analyses performed on stained thin sections (Table 1) indicate 45–67% plagioclase, 15–24% quartz,

generally less than 3% alkali feldspar, 5–16% amphibole, and less than 5% biotite. The color index varies from 8.6 to 27.5, but is mainly in the range 13–22. Accessory minerals include opaque minerals, zircon, apatite, allanite and sphene. Epidote, chlorite and sericite are secondary minerals. Plagioclase is euhedral to subhedral, compositionally zoned, and shows alteration to epidote and sericite in the inner zones. Amphibole is also euhedral to subhedral, weakly altered to epidote and chlorite, and contains frequent inclusions of opaque minerals and apatite. Biotite and alkali feldspar are irregularly distributed, the latter being absent in areas with higher enclave concentration. Alkali feldspar surrounds plagioclase, and shows a microperthitic texture. Alkali feldspar occasionally grows interstitially, and together with quartz is irregularly distributed.

Trondhjemitites are pinkish gray, and contain lesser amounts of plagioclase, amphibole and biotite, and greater amounts of quartz and alkali feldspar than tonalites

Las Matras Block (Southernmost Cuyania terrane)		
Sedimentary Cover	<p>Agua Escondida Formation Shallow marine non-fossiliferous quartz arenites, with subvertical to steeply dipping beds. Exposures in close association with those of the San Jorge Formation. Timing of deposition: Late Carboniferous? Ordovician?</p> <p>San Jorge Formation Microbialitic carbonate deposits, with thin K-rich tuff levels interbedded. Folded and partially metamorphosed to crystalline limestones (low-grade metamorphism). Cambrian to Early Ordovician deposition (Pb-Pb and U-Pb isochrons, $^{87}\text{Sr}/^{86}\text{Sr}$ compositions, conodonts).</p>	
Grenvillian basement	<p>Las Matras Pluton</p> <p><u>Geology:</u> Undeformed, microgranitoid enclave pluton. 4 km x 4 km outcrop. Country rock not exposed. Composition: trondhjemitites to tonalites.</p> <p><u>Final emplacement level:</u> Shallow. 1.9–2.6 kb</p> <p><u>Geochemistry:</u> Low-Al TTG series, low Sr/Y, low La/Yb_n. Continental & Island arc association. Sodic plagioclase and alkali feldspar.</p> <p><u>Isotopic constraints:</u> U-Pb zircon (trondhjemitite): 1244 ± 42 Ma Rb-Sr whole rock isochron: 1212 ± 47 Ma, initial $^{87}\text{Sr}/^{86}\text{Sr}$ 0.7030 ± 0.0004 EpsilonSr₍₁₂₄₄₎: -3 Sm-Nd whole rock-amphibole isochron: 1178 ± 47 Ma EpsilonNd₍₁₂₄₄₎: +2.0 K-Ar amphibole (tonalites): 869 ± 17 Ma - 750 ± 30 Ma wr (tonalites): 690 ± 20 Ma K-Ar whole rock (trondhjemitites): 392–382 Ma</p>	<p><i>Other possible Grenvillian basement:</i></p> <p>Cerro Las Pacas Formation About 35°45' S - 68°45' W. Micaschists and migmatites. Outcrop area: 2 km x 2 km.</p> <p>YPF IV-D Well data: About 36°05' S - 67° 55' W. Garnetiferous hornblende-biotite schists. K-Ar 605 Ma</p>

Fig. 2. Main geological features of the Las Matras Block. See text for data source.

(Table 1). The leucocratic character of the trondhjemites is reflected in a color index varying mainly between 3.1 and 5.5. Despite their general medium- to fine-grained granular to porphyritic textures, some areas show conspicuous granophyric textures. In these areas euhedral phenocrysts of amphibole (up to 5 mm) appear together with plagioclase. Granophyric intergrowths of quartz and alkali feldspar radially surround small euhedral plagioclase crystals. In areas with scarce granophyric intergrowths, plagioclase phenocrysts are markedly zoned and have homogeneous albite rims, whereas groundmass plagioclase grains are smaller, sub- to anhedral, and unzoned. The alkali feldspar forms part of the groundmass as subhedral crystals with scarce microperthite. Biotite has an irregular distribution, either as replacement of amphibole or as aggregates of small flakes. Quartz is poikilitic and surrounds the groundmass mineral grains.

The compositions of a few minerals were analyzed in order to (1) obtain a better knowledge of the compositions of the two facies of the pluton, and (2) have an appraisal of its emplacement level. The analyses were carried out at the Electron Microprobe Laboratory (São Paulo University, Brazil), with a JEOL-SUPERPROBE JXA-8600 S electron microprobe. The analytical conditions were a

beam current of 20.10 ± 0.10 nA and an acceleration voltage of 15.00 kV. The probe diameter was 10 μm for alkali feldspar and plagioclase, and 5 μm for amphibole.

Fresh alkali feldspar and plagioclase crystals from two representative samples (trondhjemite LMT-7 and tonalite LMT-17), and amphibole crystals from the same tonalite were analyzed (Tables 2, 3 and 4). The amphibole of the trondhjemite was not analyzed because of its scarcity and altered condition.

The optical zoning identified in the plagioclase phenocrysts of the trondhjemite was confirmed with the microanalytical data. The phenocrysts are composed of andesine ($\text{Ab}_{62-70} \text{An}_{28-36} \text{Or}_{1.5-2.4}$), with reverse zoning (cores more sodic than rims) (Table 2). In addition, the outermost rim has a homogeneous, truly albitic composition ($\text{Ab}_{90-93} \text{An}_{06-08} \text{Or}_{<01}$). The groundmass plagioclase has compositions generally similar to the albite rims, although the cores are slightly more calcic (oligoclase, $\text{Ab}_{82} \text{An}_{16} \text{Or}_{02}$) than the rims (albite, $\text{Ab}_{90} \text{An}_{09} \text{Or}_{01}$). This suggests a slight normal zoning not recognized optically. Overall, the compositional variations of plagioclase in the phenocrysts and groundmass of the trondhjemite suggest a late-stage Na-enrichment, with stabilization of a more sodic plagioclase in the groundmass than in the

Table 1. Modal analysis of tonalites and trondhjemites of the Las Matras pluton.

	Tonalitic facies									
	LMT-2	LMT-10	LMT-12	LMT-13	LMT-17	LMT-19	LMT-21	LMT-27	LMT-28t	LMT-28d
Quartz	16.2	23.4	20.8	32.6	21.9	20.2	20.3	18.3	24.1	15.4
Alkali feldspar	-	1.5	-	3.6	2.9	1.0	7.2	-	-	3.0
Plagioclase	62.4	53.5	45.2	55.2	58.9	54.2	56.9	64.4	63.2	67.5
Biotite	-	3.5	5.4	5.0	5.4	3.5	-	-	-	-
Amphibole	16.1	12.5	18.5	1.3	9.2	15.0	10.4	5.1	6.8	8.5
Epidote	0.9	0.9	1.5	1.2	1.0	4.6	1.7	tr	tr	tr
Opaque	2.4	0.8	0.5	0.3	0.6	0.4	0.7	3.1	2.2	1.8
Zircon	-	tr	tr	tr	tr	tr	tr	tr	tr	tr
Apatite	0.6	tr	tr	tr	tr	0.3	0.6	1.0	1.0	tr
Chlorite	1.4	4.0	7.6	0.8	0.1	0.8	2.2	5.4	2.6	3.8
Allanite	-	-	tr	-	-	-	-	-	-	tr
Sphene	-	-	-	-	-	-	-	-	-	-

	Trondhjemitic facies									
	LMT-1	Conspicuous granophyric texture				Scarce granophyric texture				
		LMT-6	LMT-14	LMT-15	LMT-22	LMT-7	LMT-9	LMT-11	LMT-24	LMT-25
Quartz	36.1	28.1	33.4	32.5	37.8	30.2	30.8	32.7	38.6	36.7
Alkali feldspar	30.7	34.4	28.9	27.7	25.3	23.6	23.9	19.5	24.5	27.1
Plagioclase	30.1	28.6	32.1	31.9	34.7	36.3	41.2	41.9	34.4	32.2
Biotite	-	-	2.9	2.6	0.2	6.5	1.0	3.7	-	0.7
Amphibole	-	6.5	0.3	0.1	0.3	-	0.1	-	0.4	-
Epidote	0.9	0.2	0.3	0.1	0.1	1.0	1.2	1.2	tr	1.3
Opaque	0.8	1.0	0.5	tr	0.5	0.2	0.3	0.4	0.6	0.4
Zircon	tr	tr	tr	tr	tr	0.1	tr	0.1	tr	tr
Apatite	tr	tr	tr	tr	tr	tr	tr	tr	tr	0.1
Chlorite	1.4	1.2	1.5	0.4	1.1	2.1	1.5	0.9	1.5	1.5
Allanite	tr	-	tr	-	tr	tr	-	tr	-	tr
Sphene	-	-	-	-	-	tr	-	-	-	tr

phenocrysts. A similar Na-enrichment is also seen in the groundmass alkali feldspars crystallized together with plagioclase (Table 3), as these alkali feldspars exhibit albite-enriched rims ($\text{Ab}_{24-27}\text{An}_{00-01}\text{Or}_{72-74}$) compared to the more potassic cores ($\text{Ab}_{06-07}\text{An}_{00}\text{Or}_{93-94}$). The presence of these compositional variations among alkali feldspars is also apparent in the microanalysis of perthites, where the potassic member has an albite-rich ($\text{Ab}_{61}\text{An}_{01}\text{Or}_{38}$) composition.

The plagioclases of the tonalites are normally zoned (Table 2). The inner zones vary between andesine ($\text{Ab}_{57-69}\text{An}_{29-42}\text{Or}_{01-02}$) and oligoclase ($\text{Ab}_{78}\text{An}_{19}\text{Or}_{03}$), and the outer zones between oligoclase ($\text{Ab}_{74-86}\text{An}_{12-25}\text{Or}_{00-01}$) and albite ($\text{Ab}_{95}\text{An}_{04}\text{Or}_{01}$). The sodium enrichment of the rims is equivalent to the late-stage albitic rims of the trondhjemites, confirming the common origin of the two facies proposed on the basis of whole rock geochemistry. The only alkali feldspar analyzed from tonalite shows a slightly reversed alkali zoning variation with respect to the trondhjemites, with core composition $\text{Ab}_{08}\text{An}_{00}\text{Or}_{92}$ and rim composition $\text{Ab}_{04}\text{An}_{00}\text{Or}_{96}$ (Table 3).

The amphiboles of the tonalites have a complex chemical composition. According to the classification of Leake et al. (1997), they belong to the calcic amphibole group, with $(\text{Ca} + \text{Na})_{\text{B}} \geq 1.0$; $\text{Ca}_{\text{B}} \geq 1.5$ and $\text{Na}_{\text{B}} \leq 0.5$ (Table 4). Within this group the amphiboles are further classified into two subgroups, one with $(\text{Na} + \text{K})_{\text{A}} < 0.5$ and $\text{Ca}_{\text{A}} < 0.5$, and the other with $(\text{Na} + \text{K})_{\text{A}} \geq 0.5$ and $\text{Ti} < 0.5$. The first subgroup corresponds to ferrohornblendes with Si between 6.9 and 7.1 apfu, and Mg# (Mg/Mg+Fe) between 0.48 and 0.50. The amphiboles of the second subgroup are ferroedenites with Si between 6.5 and 7.1 apfu, and Mg# between 0.44 and 0.47. In all cases the amphiboles do not show any definite zoning pattern.

Geothermometry and geobarometry calculations were performed for the tonalite sample LMT-17 with the above mentioned chemical results. Hornblende-plagioclase pairs were used for temperature calculation (quartz calibration after Holland and Blundy, 1994, at reference pressure 1 kb, amphibole with $\text{Na}_{\text{A}} > 0.02$ pfu, $\text{Al}^{\text{VI}} < 1.8$ pfu and Si range 6.0–7.7 pfu, and plagioclase with $X_{\text{An}} < 0.9$; see Tables 2 and 4), and the Al-in-amphibole barometer was used for pressure calculation (calibration of Anderson and Smith, 1995, for amphibole with Fe/Fe+Mg range 0.40–0.65; see Table 4). The pressure values obtained for rims and cores vary between 1.9 and 2.6 (± 0.6) kb (for the mean minimum temperature of 710° C, see below), indicating a shallow depth of emplacement for the Las Matras pluton. However, one value of 4.7 ± 0.6 kb from a core analysis might indicate a more complex emplacement history, with ascent from deeper levels.

Sphene is lacking from sample LMT-17, but Anderson

and Smith (1995) point out that the absence of sphene from the assemblage quartz + alkali feldspar + plagioclase + amphibole + biotite + iron-titanium oxide does not appear to significantly affect pressure determinations. However, it is noted here that the temperature calculations were performed using the recommendation of Johnson and Rutherford (1989) ($X_{\text{An}} < 0.9$) rather than the narrower range ($X_{\text{An}} 0.25\text{--}0.30$) of Anderson and Smith (1995), a situation that might introduce some uncertainty.

With regard to the temperature calculations, they are not considered conclusive because of the complex compositional variations of the plagioclase and amphibole. Despite that, a mean minimum cooling temperature of $\sim 710^\circ\text{C}$ was calculated, and we consider that the crystallization temperatures should be above this value.

To summarize, the sodic character of both the plagioclase and alkali feldspar in the tonalite and in the trondhjemite is in full agreement with the bulk chemical composition in indicating these rocks are part of a tonalite-trondhjemite-granodiorite or TTG series. The shallow depth derived for the final emplacement level of the Las Matras pluton (1.9 to 2.6 ± 0.6 kb) is in agreement with the shallow level of emplacement for rocks with granophyric and porphyritic textures.

Zircon U-Pb Dating

A sample of the trondhjemitic facies (sample LMT-31, with 71.6% SiO_2 ; Sato et al., 2000) was chosen for conventional zircon U-Pb dating. The analyses were carried out at the Centro de Pesquisas Geocronológicas, São Paulo University (Brazil). Zircons were separated from crushed, bulk rock samples, with standard heavy liquid, magnetic splitting and hand picking techniques (Basei et al., 1995). A mixed $^{205}\text{Pb}/^{235}\text{U}$ spike was added to each zircon fraction and then digested in Teflon microcapsules with a mixture of HF and HNO_3 , at 200°C for 72 hours. Separation and purification of U and Pb were performed in cation exchange columns, following the technique described by Krogh (1973). A Finnigan MAT 262 multi-collector mass spectrometer was used for isotopic ratio measurements. During the period of analyses the mean values of $^{207}\text{Pb}/^{206}\text{Pb}$ ratios were: NBS 983: 0.071212 ± 0.000035 ; NBS 981: 0.91479 ± 0.000094 ; and NBS 982: 0.46692 ± 0.000047 (Sato and Kawashita, 2002). The U and Pb concentrations as well as the $^{207}\text{Pb}/^{235}\text{U}$, $^{206}\text{Pb}/^{238}\text{U}$ and $^{207}\text{Pb}/^{206}\text{Pb}$ ratios were calculated with the PBDAT software. The age calculation and concordia diagrams were based on Isoplot/Ex program (Ludwig, 1998).

Four magnetic fractions of zircons were analyzed (Table 5 and Fig. 3). Zircon crystals are light brown, euhedral and prismatic (axial ratios 2:1 to 1:1), with

Table 2. Selected electron probe microanalyses of plagioclase from trondhjemite LMT-7 and tonalite LMT-17.

Wt%	Trondhjemite LMT-7								
	Phenocryst 1				Phenocryst 2			Groundmass	
	Outer rim	Inner rim	Core	Core	Outer rim	Core	Core	Core	Core
SiO ₂	66.403	60.359	60.239	60.775	65.414	59.051	58.756	65.666	63.506
TiO ₂	0.025	0.028	0.014	0.000	0.001	0.000	0.000	0.007	0.045
Al ₂ O ₃	20.460	24.703	24.470	23.609	20.925	25.511	25.363	20.824	22.001
Fe ₂ O ₃	0.121	0.212	0.260	0.257	0.126	0.285	0.264	0.158	0.055
MnO	0.001	0.008	0.006	0.000	0.005	0.000	0.024	0.005	0.013
MgO	n.a.	0.032	0.006	0.004	0.005	0.000	0.000	0.000	0.011
CaO	1.403	6.697	6.238	5.814	1.921	7.549	7.395	1.915	3.417
SrO	n.a.	0.027	0.106	0.022	0.000	0.016	0.045	0.000	0.002
BaO	0.041	0.068	0.045	0.000	0.082	0.022	0.000	0.000	0.129
Na ₂ O	11.219	7.881	7.988	8.041	10.702	7.187	7.414	10.856	9.815
K ₂ O	0.112	0.373	0.404	0.417	0.098	0.263	0.315	0.213	0.297
Total	99.79	100.38	99.78	98.94	99.28	99.88	99.58	99.65	99.29
	cations per 32 oxygens								
Si	11.700	10.741	10.779	10.9327	11.597	10.570	10.563	11.606	11.323
Al	4.249	5.181	5.161	5.0054	4.372	5.382	5.374	4.338	4.623
Ti	0.003	0.004	0.002	0.0000	0.000	0.000	0.000	0.001	0.006
Fe ³⁺	0.016	0.028	0.035	0.0348	0.017	0.038	0.036	0.021	0.007
Mn	0.000	0.001	0.001	0.000	0.001	0.000	0.004	0.001	0.002
Mg	0.000	0.009	0.002	0.001	0.001	0.000	0.000	0.000	0.003
Ca	0.265	1.277	1.196	1.120	0.365	1.448	1.424	0.363	0.653
Na	3.833	2.719	2.771	2.804	3.679	2.495	2.584	3.720	3.393
K	0.025	0.085	0.092	0.096	0.022	0.060	0.072	0.048	0.069
Ba	0.003	0.005	0.003	0.000	0.006	0.002	0.000	0.000	0.009
Sr	0.000	0.003	0.011	0.002	0.000	0.002	0.005	0.000	0.000
sum X	4.126	4.098	4.076	4.024	4.073	4.006	4.089	4.132	4.127
sum Z	15.968	15.954	15.977	15.973	15.986	15.991	15.972	15.966	15.959
total	20.094	20.052	20.053	19.997	20.059	19.997	20.061	20.098	20.087
An	6.42	31.29	29.46	27.87	8.97	36.17	34.90	8.78	15.87
Ab	92.96	66.63	68.27	69.75	90.48	62.32	63.32	90.06	82.49
Or	0.61	2.08	2.27	2.38	0.55	1.50	1.77	1.16	1.64
	Tonalite LMT-17								
Wt%	Crystal 1			Crystal 2			Crystal 3		
	Rim	Core	Rim	Rim	Core	Rim	Rim	Core	Rim
SiO ₂	64.275	59.977	60.092	62.816	56.375	66.491	64.125	63.111	65.596
TiO ₂	0.034	0.000	0.020	0.000	0.074	0.017	0.034	0.015	0.034
Al ₂ O ₃	21.720	24.370	23.442	22.517	26.429	20.291	22.036	22.530	19.818
Fe ₂ O ₃	0.224	0.215	0.158	0.247	0.200	0.184	0.114	0.176	0.899
MnO	0.000	0.000	0.011	0.000	0.000	0.028	0.014	0.023	0.024
MgO	0.007	0.000	0.010	0.029	0.017	0.012	0.000	0.000	0.000
CaO	3.022	6.168	5.381	3.912	8.708	0.966	2.966	3.773	2.634
SrO	0.000	0.000	0.034	0.049	0.121	0.002	0.033	0.027	0.015
BaO	0.235	0.063	0.143	0.223	0.121	0.069	0.418	0.213	0.072
Na ₂ O	10.052	8.154	8.681	9.667	6.590	11.574	10.126	9.165	9.973
K ₂ O	0.270	0.269	0.090	0.117	0.251	0.147	0.109	0.568	0.147
total	99.84	99.22	98.06	99.58	98.89	99.78	99.97	99.60	99.21
	cations per 32 oxygens								
Si	11.395	10.783	10.915	11.198	10.260	11.723	11.359	11.240	11.666
Al	4.538	5.164	5.018	4.731	5.669	4.216	4.601	4.729	4.154
Ti	0.005	0.000	0.003	0.000	0.010	0.002	0.005	0.002	0.005
Fe ³⁺	0.030	0.029	0.0215	0.033	0.027	0.024	0.015	0.024	0.120
Mn	0.000	0.000	0.002	0.000	0.000	0.004	0.002	0.004	0.004
Mg	0.002	0.000	0.003	0.008	0.005	0.003	0.000	0.000	0.000
Ca	0.574	1.188	1.047	0.747	1.698	0.183	0.563	0.720	0.502
Na	3.455	2.842	3.057	3.341	2.325	3.956	3.478	3.165	3.439
K	0.061	0.062	0.021	0.027	0.058	0.033	0.025	0.129	0.033
Ba	0.016	0.005	0.010	0.016	0.009	0.005	0.029	0.015	0.005
Sr	0.000	0.000	0.004	0.005	0.013	0.000	0.003	0.003	0.002
sum X	4.108	4.096	4.144	4.143	4.108	4.184	4.100	4.035	3.984
sum Z	15.967	15.976	15.958	15.961	15.966	15.966	15.980	15.994	15.944
total	20.075	20.072	20.101	20.105	20.074	20.149	20.080	20.029	19.929
An	14.03	29.04	25.38	18.16	41.60	4.37	13.85	17.94	12.63
Ab	84.47	69.46	74.11	81.20	56.97	94.83	85.55	78.85	86.53
Or	1.49	1.51	0.51	0.64	1.43	0.79	0.61	3.22	0.84

Table 3. Selected electron probe microanalyses of alkali feldspar from trondhjemite LMT-7 and tonalite LMT-17.

Wt%	Trondhjemite LMT-7				Tonalite LMT-17		
	Rim	Core	Rim	Perthite	Rim	Rim	Core
SiO ₂	63.717	63.040	63.261	64.770	63.553	63.119	64.116
TiO ₂	0.008	0.000	0.000	0.060	0.003	0.028	0.028
Al ₂ O ₃	18.523	18.100	18.154	18.945	18.775	18.130	18.282
Fe ₂ O ₃	0.147	0.080	0.000	0.000	0.017	0.192	0.018
MnO	0.005	0.000	0.010	0.015	0.033	0.000	0.000
CaO	0.100	0.000	0.000	0.295	0.220	0.014	0.027
BaO	0.108	0.265	0.207	0.367	0.574	0.405	0.510
Na ₂ O	3.141	0.753	0.677	7.325	2.715	0.386	0.840
K ₂ O	12.726	15.785	16.172	6.759	12.346	16.277	15.437
Cl	0.038	0.063	0.021	0.093	na	0.080	0.002
Total	98.512	98.087	98.502	98.628	98.238	98.632	99.259
cations per 32 oxygens							
Si	11.877	11.932	11.931	11.8432	11.870	11.918	11.963
Al	4.069	4.038	4.035	4.0827	4.133	4.035	4.020
Ti	0.001	0.000	0.000	0.0083	0.000	0.004	0.004
Fe ³⁺	0.021	0.011	0.000	0.0000	0.002	0.027	0.003
Mn	0.001	0.000	0.002	0.002	0.005	0.000	0.000
Ca	0.020	0.000	0.000	0.058	0.044	0.003	0.005
Na	1.135	0.277	0.247	2.597	0.983	0.141	0.304
K	3.026	3.811	3.891	1.577	2.942	3.921	3.675
Ba	0.008	0.020	0.015	0.026	0.042	0.030	0.037
Cl	0.012	0.020	0.007	0.029	0.000	0.026	0.001
sum X	4.202	4.128	4.162	4.288	4.016	4.120	4.022
sum Z	15.968	15.981	15.966	15.934	16.006	15.984	15.990
total	20.170	20.108	20.128	20.223	20.023	20.104	20.0126
An	0.48	0.00	0.00	1.36	1.11	0.07	0.13
Ab	27.15	6.76	5.98	61.38	24.77	3.47	7.63
Or	72.38	93.24	94.02	37.26	74.12	96.46	92.24

abundant mineral inclusions and fractures. Despite the small variation in U contents, the analyzed fractions define a good discordia line (MSWD 3.3) with an upper intercept at 1244 ± 42 Ma. This date is consistent with the previous Rb-Sr and Sm-Nd isochron within errors, and is interpreted as the crystallization age of the pluton. This age is only slightly older than that proposed by Sato et al. (2000).

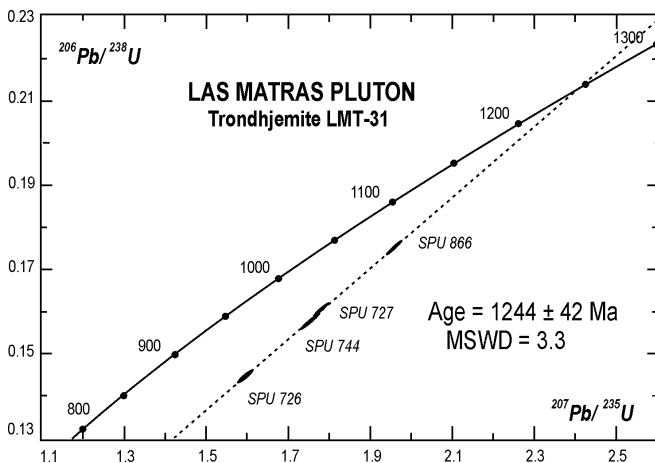


Fig. 3. U-Pb Concordia diagram for the trondhjemitic facies of the Las Matras pluton, based on Ludwig (1998).

Table 4. Selected electron probe microanalyses of amphibole from tonalite LMT-17. (*) Calibration of Anderson and Smith (1995) using a mean minimum temperature of 710° C.

Wt%	Tonalite LMT-17					
	Rim	Core	Rim	Rim	Core	Rim
SiO ₂	46.604	45.675	46.706	46.500	43.145	46.703
TiO ₂	1.016	1.632	1.421	1.387	2.612	1.412
Al ₂ O ₃	6.308	7.150	6.330	6.403	9.760	6.651
FeO	20.814	19.412	19.382	20.611	20.611	19.678
MnO	0.556	0.402	0.461	0.348	0.352	0.362
MgO	10.345	10.142	10.927	10.354	9.238	10.188
CaO	10.201	10.762	10.329	10.566	10.654	10.828
Na ₂ O	1.331	1.508	1.467	1.892	2.391	0.677
K ₂ O	0.615	0.368	0.544	0.392	0.366	0.439
F	0.249	0.348	0.310	0.754	0.749	0.037
Cl	0.264	0.145	0.207	0.177	0.100	0.207
Total	98.30	97.55	98.08	99.38	99.98	97.18
cations per 23 oxygens						
Si	7.061	6.940	7.046	7.000	6.497	7.077
Al ^{IV}	0.939	1.060	0.954	1.000	1.503	0.923
sum T	8.000	8.00	8.000	8.000	8.000	8.000
Al ^{VI}	0.188	0.221	0.171	0.137	0.229	0.265
Ti	0.116	0.187	0.161	0.157	0.296	0.161
Mg	2.337	2.297	2.457	2.324	2.074	2.302
Fe ²⁺	2.360	2.295	2.210	2.383	2.402	2.272
sum C	5.00	5.000	5.000	5.000	5.000	5.000
Fe ²⁺	0.277	0.171	0.235	0.212	0.194	0.222
Mn	0.071	0.052	0.0590	0.044	0.045	0.046
Ca	1.656	1.752	1.670	1.704	1.719	1.758
Na	0.000	0.025	0.037	0.039	0.043	0.000
sum B	2.005	2.000	2.000	2.000	2.000	2.026
Na	0.391	0.419	0.393	0.513	0.656	0.199
K	0.119	0.071	0.105	0.075	0.070	0.085
sum A	0.510	0.491	0.497	0.588	0.726	0.284
total	15.515	15.491	15.497	15.588	15.726	15.310
Mg/(Mg+Fe)	0.470	0.482	0.501	0.472	0.444	0.480
Fe/(Fe+Mg)	0.530	0.518	0.499	0.528	0.556	0.520
Al-in-hornblende barometry: $P \pm 0.6$ kb (*)						
	1.92	2.62	1.92	1.96	4.67	2.20

The T_{DM} model ages given in Sato et al. (2000) are recalculated here with this new crystallization age, following DePaolo et al. (1991). The recalculated model ages range from 1604 to 1613 Ma, and differ only marginally from the previously reported ages (1551 to 1605 Ma). Neither the $\zeta Nd(t)$ nor the $\zeta Sr(t)$ varies greatly, from +1.6 ~ +1.8 to +2.0 ~ +2.1, and from -4.5 ~ +4.8 to -10.7 ~ -3.4, respectively, and confirm the depleted character of the source. Thus both the age interpretation and the isotopic characterization given in Sato et al. (2000) are not substantially modified by these new data.

Discussion

The new data presented in this study in combination with the already published information in Sato et al. (2000) suggest that the Las Matras pluton was emplaced at 1244 ± 42 Ma, and forms part of a low-Al TTG suite (tonalites to trondhjemites) intruded at a shallow level constrained between 1.9 and 2.6 kb.

Sato et al. (2000) noted that a crystallization age of around 1200 Ma was slightly older (by about 100 m.y.) than those obtained for the Grenville-aged rocks to the north. However, more recent studies have found that similar zircon U-Pb ages are much more common in the Cuyania terrane, such as in the Sierra de Umango (Varela et al., 2003a), the Sierra de Pie de Palo (Vujovich et al., 2004, this volume) and the San Rafael Block (Cingolani et al., in prep.), suggesting a longer Grenvillian history than previously considered. An extended Grenvillian history is also supported by reports of numerous younger isotopic ages of ca. 1000 Ma (Varela and Dalla Salda, 1992; McDonough et al., 1993; Abruzzi et al., 1993; Mahlburg Kay et al., 1996; Pankhurst and Rapela, 1998). All areas of Cuyania basement also share common Nd-Sr depleted features and Mesoproterozoic T_{DM} ages (Mahlburg Kay et al., 1996; Cingolani and Varela, 1999; Porcher et al., 2003; Varela et al., 2003b).

If the Las Matras basement and the nearby San Rafael Block are compared, some similarities as well as some differences are noted. The similarities are: comparable U-Pb age and TTG character (Cingolani et al., in prep.), and similar low-Rb and moderate-Sr contents (Cingolani and Varela, 1999) of the dated rocks. The San Rafael Block differs with respect to the Las Matras Block in the existence of metamorphic rocks (e.g., amphibolites, quartz micaschists, metaquartzites, and gneisses, Núñez, 1979) that might represent a country rock for the granodioritic to tonalitic rocks dated by Cingolani and Varela (1999). According to the descriptions of Núñez (1979), the magmatic textures of the tonalites in the San Rafael Block are overprinted by a mylonitic ductile deformation (recrystallized quartz, curved plagioclase twins), a tectonic feature also stressed by Criado Roqué and Ibáñez (1979), even though its timing is uncertain. Although the outcrops of the Las Matras pluton cover a slightly smaller area (4 km by 4 km) than those of the Cerro Ventana Formation (10 km by 2 km), no signs of ductile deformation were found in Las Matras. Taking into account that all the Grenvillian basement rocks to the north of San Rafael Block is affected by at least two orogenic deformations

associated with high-grade metamorphism (Casquet et al., 2001; Varela et al., 2003a; Porcher et al., 2003; Vujovich et al., 2004 this volume), they are interpreted to represent deeper crustal levels relative to Las Matras area. This suggests a shallower crustal level is exposed toward the south. Within this context, the undeformed feature of the Las Matras pluton might be explained as either a result of strain heterogeneity at low to medium metamorphic grade, or alternatively, a local tectonic setting that protected the area from regional deformation. In any case, the small outcrop size precludes any regional interpretation of this distinctive characteristic.

Our interpretation of the Early Paleozoic regional tectonic setting is depicted in figure 1, where we show the Cuyania terrane accreted to the western margin of Gondwana, and the collisional Famatinian orogeny affecting both terranes. Although the Famatinian magmatic arc granitoids intrude only into the Gondwana margin, the deformational and metamorphic effects related to collision are shown with a variable degree of intensity both across and along the orogen. The strongest compressive effects are reported around the suture zone between Sierra de Pie de Palo and Sierra de la Huerta, with high-pressure metamorphism (Casquet et al., 2001; Baldo et al., 2001); a transition to low-pressure conditions is apparent toward the east and reaching the Sierra de Chepes (Baldo et al., 2001). To the southeast of Sierra de Chepes, the high-grade regional metamorphism related to collision is of medium-pressure (Barrovian-type) in Sierra de San Luis, and the associated penetrative deformation has almost entirely erased previous structures (González et al., 2004, this volume). However, the regional metamorphic effects did not reach the Sierra de Córdoba at these latitudes, where only ductile shear zones and scarce magmatism are found in relation to the Ordovician (Rapela et al., 1998; Bonalumi and Baldo, 2002; Simpson et al., 2003). Further south at the latitudes of Las Matras Block, the Ordovician metamorphic rocks of the Chadileuvú Block comprise very low- to medium-grade rocks (Linares et al., 1980; Tickyj, 1999; Tickyj et al., 2002) and are intruded by granitoids (Tickyj et al., 1999). Despite

Table 5. U-Pb analytical data of trondhjemite LMT-31.

	Magnetic Fraction (1)	Weight (ug)	U (ppm)	Pb (ppm)	$^{206}\text{Pb}/^{204}\text{Pb}$ Observed (3)	$^{206}\text{Pb}/^{238}\text{U}$ (4)	Error (%)	$^{207}\text{Pb}/^{235}\text{U}$ (4)	Error (%)	$^{207}\text{Pb}/^{206}\text{Pb}$ (4)	Error (%)	Age (5)		
												$^{206}\text{Pb}/^{238}\text{U}$	$^{207}\text{Pb}/^{235}\text{U}$	$^{207}\text{Pb}/^{206}\text{Pb}$
SPU727	M(-2)	0.063	363.7	58.0	885.4	0.144549	1.040	1.59554	1.140	0.080055	0.458	870	968	1198
SPU726	M(-3)	0.077	213.4	37.4	876.1	0.160491	0.864	1.77898	0.894	0.080393	0.228	960	1038	1207
SPU744	M(-1)	0.056	316.9	58.1	502.9	0.157577	1.060	1.75262	1.110	0.080667	0.333	943	1028	1213
SPU866	NM(-3)	0.054	320.8	58.1	2325.9	0.175177	0.671	1.95931	0.700	0.081119	0.201	1041	1102	1224

SPU: Laboratory number; (1) Magnetic fractions; numbers in parenthesis indicate the tilt used on Frantz separator at 1.5 amp current; (2) Total U and Pb concentrations corrected for analytical blank; (3) Not corrected for blank or non-radiogenic Pb; (4) Radiogenic Pb corrected for blank and initial Pb; U corrected for blank; (5) Ages given in Ma, after Isoplot/Ex Program (Ludwig, 1998), decay constants recommended by Steiger and Jäger (1977).

the evidence for Ordovician metamorphism and deformation in the Chadileuvú Block, the Cambro-Ordovician San Jorge Formation in the adjacent Las Matras Block exhibits only partial low-grade metamorphism, and the Las Matras pluton is completely free of metamorphism. The question how the Las Matras pluton survived the effects of both the Grenvillian and Famatinian deformation is unresolved. At least in the case of the younger collisional Famatinian orogeny, we suspect a decrease in the regional compressive effects toward the south (Sato et al., 2003), perhaps in relation to some geometrical changes in the subduction configuration.

The continuity of the Cuyania terrane further south into the Patagonia was not confirmed (Sato et al., 2000), and high-resolution aeromagnetic data suggest this terrane was truncated south of 39°S (Chernicoff and Zappettini, 2003). However, it is striking that evidence of the Famatinian orogen apparently continues to the south, with Ordovician arc magmatism, metamorphism and deformation at scattered locations within the North-Patagonian Massif (Varela et al., 1997, 1998; Pankhurst et al., 2001; Rapela and Pankhurst, 2002) and the Deseado Massif (Pankhurst et al., 2003). Even though Patagonia was proposed to be allochthonous by Ramos (1984), this matter remains in debate. An unresolved issue is that the structural orientations in the southern regions do not completely coincide with those to the north, although this situation might be the result of a subsequent late Paleozoic ductile overprint, which is recognized in the North-Patagonian region (e.g., Llambías et al., 2002). Present knowledge does not permit us to give a conclusive opinion, but determining whether the southern extension of the Famatinian orogeny in Patagonia was of a collisional type or not could contribute significantly to our understanding of the relationship between Patagonia and the rest of Gondwana.

Concluding Remarks

A zircon U-Pb age of 1244 ± 42 Ma obtained for the Las Matras pluton fits well with current geochronological knowledge of the Grenvillian basement rocks in the Cuyania terrane. Together with the subsequent metamorphic processes, the Grenvillian history of the Cuyania basement is documented through more than 200 million years (up to ca. 1000 Ma).

The tonalitic to trondhjemitic composition of the Las Matras pluton is confirmed by the Na-rich compositions of the feldspars, and amphibole compositions constrain the final emplacement level in the range of 1.9 to 2.6 kb. This shallow level of emplacement is also documented by the common granophyric textures. On a regional scale, the Cuyania basement exposes shallower crustal levels to the south.

Within the collisional Famatinian orogen, the northern regions of the Cuyania basement are more strongly involved in the compressive deformation related to collision than the southern regions, and thus they exhibit two superposed deformations. In the adjacent autochthonous regions the regional metamorphism grade decreases toward the east. In contrast and to the south, the Las Matras Block lacks significant deformation, and this fact suggests that neither the Grenvillian nor the Famatinian orogeny have significantly affected it. However, in the adjacent and autochthonous Chadileuvú Block, the Famatinian orogeny overprinted a low- to medium-grade metamorphism and produced a magmatic arc similar to that found in the north.

Although outcrops displaying equivalent evidence for the magmatic, metamorphic and deformational signatures of the Famatinian orogen are well documented further south in the Patagonia, the expected continuity of the Cuyania terrane south of Las Matras Block remains uncertain.

Acknowledgments

We wish to thank R. Varela and C. Cingolani for helpful discussions about regional interpretations. We are grateful to the reviewers, V. Ramos and P. Gromet, whose comments contributed to improve the manuscript. The final English version was greatly benefited by the kind assistance of P. Gromet. Field and laboratory work were financially supported by Conicet (Grant PIP 4329/96), ANPCyT (Grant PICT 0743) and UNLP.

References

- Abruzzi, J.M., Kay, S.M. and Bickford, M.E. (1993) Implications for the nature of the Precambrian basement from the geochemistry and age of Precambrian xenoliths in Miocene volcanic rocks, San Juan province. 12° Cong. Geol. Argentino, Actas 3, pp. 331-339.
- Aceñolaza, F.G. and Toselli, A.J. (1976) Consideraciones estratigráficas y tectónicas sobre el Paleozoico interior del Noroeste Argentino 2° Cong. Latinoamericano Geol., Actas 2, pp. 755-763.
- Anderson, J.L. and Smith, D.R. (1995) The effects of temperature and f_{O_2} on the Al-in-hornblende barometer. *Amer. Mineral.*, v. 80, pp. 549-559.
- Astini, R., Benedetto, J.L. and Vaccari, N.E. (1995) The Early Paleozoic evolution of the Argentine Precordillera as a Laurentian rifted, drifted, and collided terrane: A geodynamic model. *Geol. Soc. Amer., Bull.*, v. 107, pp. 253-273.
- Baldo, E., Casquet, C., Rapela, C.W., Pankhurst, R.J., Galindo, C., Fanning, C.M. and Saavedra, J. (2001) Ordovician metamorphism at the southwestern margin of Gondwana: P-T conditions and U-Pb SHRIMP ages from Loma de Las Chacras, Sierras Pampeanas. 3rd South Amer. Symp. Isotope Geology, Ext. abst., on CD-ROM, Sernageomin, Santiago, pp. 544-547.

- Basei, M.A.S., Siga Junior, O., Sato, K. and Sproesser, W.M. (1995) A instalação da metodologia U-Pb na Universidade de São Paulo. Princípios metodológicos, aplicações e resultados obtidos. *Anais Acad. Brasil. Ciências*, v. 67, pp. 221-237.
- Bonalumi, A. and Baldo, E. (2002) Ordovician magmatism in the Sierras Pampeanas of Córdoba. In: Aceñolaza, F.G. (Ed.), *Aspects on the Ordovician system of Argentina*. Univ. Nac. Tucumán, INSUGEO, Serie Correlación Geológica, v. 16, pp. 243-256.
- Camino, R.L. (1979) Sierras Pampeanas Noroccidentales. Salta, Tucumán, Catamarca, La Rioja y San Juan. In: Turner, J.C.M. (Ed.), 2° Simp. Geol. Regional Argentina. *Acad. Nac. Ciencias*, Córdoba, v. 1, pp. 225-291.
- Casquet, C., Baldo, E., Pankhurst, R.J., Rapela, C.W., Galindo, C., Fanning, C.M. and Saavedra, J. (2001) Involvement of the Argentine Precordillera terrane in the Famatinian mobile belt: U-Pb SHRIMP and metamorphic evidence from the Sierra de Pie de Palo. *Geology*, v. 29, pp. 703-706.
- Chernicoff, C.J. and Zappettini, E.O. (2003) Solid geology and delimitation of terranes in the southern-central region of Argentina: geophysical evidences. *Simp. Internac. Acreção do microcontinente Cuyania à proto-margem do Gondwana*. Univ. Fed. Rio Grande do Sul, Porto Alegre, p. 3.
- Cingolani, C.A. and Varela, R. (1999) Rb-Sr isotopic age of basement rocks of the San Rafael Block, Mendoza, Argentina. 2° South Amer. Symp. Isotope Geology, Ext. abst., pp. 23-26.
- Criado Roqué, P. (1972) Cinturón Móvil Mendocino-Pampeano. In: Leanza, A.F. (Ed.), 1° Simp. Geol. Regional Argentina. *Acad. Nac. Ciencias Córdoba*, pp. 283-303.
- Criado Roqué, P. and Ibáñez, G. (1979) Provincia Geológica Sanrafaelino-Pampeana. In: Turner, J.C.M. (Ed.), 2° Simp. Geol. Regional Argentina. *Acad. Nac. Ciencias Córdoba*, v. 1, pp. 837-869.
- Criado Roqué, P. (1979) Subcuenca de Alvear (provincia de Mendoza). In: Turner, J.C.M. (Ed.), 2° Simp. Geol. Regional Argentina. *Acad. Nac. Ciencias Córdoba*, v. 1, pp. 811-836.
- DePaolo, D.J., Linn, A.M. and Schubert, G. (1991) The continental crust age distribution: methods of determining mantle separation ages from Sm-Nd isotopic data and application to the southwestern United States. *J. Geophys. Res.*, v. 96, pp. 2071-2088.
- González, P.D., Sato, A.M., Llambías, J., Basei, M.A.S. and Vlach, S.R.F. (2004) Early Paleozoic structural and metamorphic evolution of western Sierra de San Luis (Argentina), in relation to Cuyania accretion. *Gondwana Res.*, v. 7, pp. 1157-1170.
- Holland, T. and Blundy, J. (1994) Non ideal interactions in calcic amphiboles and their bearing on amphibole-plagioclase thermometry. *Contrib. Mineral. Petrol.*, v.116, pp. 433-447.
- Holmberg, E. (1973) Descripción geológica de la hoja 29d Cerro Nevado (1:200.000). *Serv. Nac. Geológico Minero*, Buenos Aires, Bol. 144, p. 71.
- Johnson, M. and Rutherford, M. (1989) Experimental calibration of the aluminum-in-hornblende geobarometer with application to Long Valley caldera (California) volcanic rocks. *Geology*, v. 17, pp. 837-841.
- Krogh, T.E. (1973) A low-contamination method for hydrothermal decomposition of zircon and extraction of U and Pb for isotopic age determinations. *Geochim. Cosmoch. Acta*, v. 37, pp. 485-494.
- Leake, B., Woolley, A., Arps, C., Birch, W., Gilbert, M., Grice, J., Hawthorne, F., Kato, A., Kisch, H., Krivovichev, V., Linthout, K., Laird, J., Mandarino, J., Maresch, W., Nickel, E., Rock, N., Schumacher, J., Smith, D., Stephenson, N., Ungaretti, L., Whittaker, E. and Youzih, G. (1997) Nomenclature of amphiboles: report of the Subcommittee on Amphiboles of the International Mineralogical Association, Commission on New Minerals and Mineral Names. *Amer. Mineral.*, v. 82, pp. 1019-1037.
- Linares, E., Llambías, E.J. and Latorre, C.O. (1980) Geología de la Provincia de La Pampa, República Argentina y geocronología de sus rocas metamórficas y eruptivas. *Rev. Asoc. Geol. Argentina*, v. 35, pp. 87-146.
- Llambías, E.J., Varela, R., Basei, M.A.S. and Sato, A.M. (2002) Deformación dúctil y metamorfismo neopaleozoico en el área de Yaminué y su relación con la Fase Orogénica San Rafael. 15° Cong. Geol. Argentino, *Actas*, 3, pp. 123-128.
- Ludwig, K.R. (1998) Using Isoplot/Ex. A geochronological toolkit for Microsoft Excel. Berkeley Geochronology Center, Spec. Pub. N° 1. Berkeley, USA.
- McDonough, M.R., Ramos, V.A., Isachsen, C.E., Bowring, S.A. and Vujovich, G. (1993) Edades preliminares de circones del basamento de la Sierra de Pie de Palo, Sierras Pampeanas occidentales de San Juan, sus implicancias para el supercontinente proterozoico de Rodinia. 12° Cong. Geol. Argentino, *Actas*, 3, pp. 340-342.
- Mahlburg Kay, S., Orrell, S. and Abbruzzi, J.M. (1996) Zircon and whole rock Nd-Pb isotopic evidence for a Grenville age and a Laurentian origin for the basement of the Precordillera in Argentina. *J. Geol.*, v. 104, pp. 637-648.
- Melchor, R.N., Cheng, Z. and Foland, K. (1999a) Isotopic dating of San Jorge Fm. limestones (Early Paleozoic): Preliminary results from a Pb/Pb isochron and ⁸⁷Sr/⁸⁶Sr ratios. 2nd S. Amer. Symp. Isotope Geol., Ext. abst., pp. 414-417.
- Melchor, R.N., Tickyj, H. and Dimieri, L.V. (1999b) Estratigrafía, Sedimentología y Estructura de la Fm. San Jorge (Paleozoico Inferior), La Pampa, Argentina. 14° Cong. Geol. Argentino, *Actas*, 1, pp. 389-392.
- Melchor, R.N., Sato, A.M., Llambías, E.J. and Tickyj, H. (1999c) Confirmación de la extensión meridional del terreno Cuyania/Precordillera en la provincia de La Pampa, Argentina. 14° Cong. Geol. Argentino, *Actas*, 1, pp. 156-159.
- Núñez, E. (1979) Descripción geológica de la hoja 28d Estación Soitué. *Serv. Nac. Geológico Minero*, Buenos Aires, Bol. 144, p. 67.
- Pankhurst, R.J., Rapela, C.W. and Fanning, C.M. (2001) The Mina Gonzalito Gneiss: Early Ordovician metamorphism in Northern Patagonia. 3rd S. Amer. Symp. Isotope Geol., Ext. abst. CD-ROM, Sernageomin, Santiago, pp. 604-607.
- Pankhurst, R.J. and Rapela, C.W. (1998) The Proto-Andean margin of Gondwana: an introduction. In: Pankhurst, R.J. and Rapela, C.W. (Eds.), *The Proto-Andean margin of Gondwana*. *Geol. Soc. Lon. Spec. Pub.*, v. 142, pp. 1-9.
- Pankhurst, R.J., Rapela, C.W., Loske, W.P., Márquez, M. and Fanning, C.M. (2003) Chronological study of the pre-Permian basement rocks of southern Patagonia. *J. S. Amer. Earth Sci.*, v. 16, pp. 27-44.
- Porcher, C.C., Fernandes, L.A.D. and Vujovich, G.I. (2003) Sm/Nd ages, thermobarometry and metamorphic evolution of the NW Sierras Pampeanas, Argentina. *Simp. Internac. Acreção do microcontinente Cuyania à proto-*

- margem do Gondwana. Univ. Fed. Rio Grande do Sul, Porto Alegre, p. 11.
- Ramos, V.A. (1984) Patagonia ¿Un continente paleozoico a la deriva? 9° Cong. Geol. Argentino, Actas, 2, pp. 311-325.
- Ramos, V.A. (1995) Sudamérica: un mosaico de continentes y océanos. *Ciencia Hoy*, v. 6, pp. 24-29.
- Ramos, V.A., Dallmeyer, R.D. and Vujovich, G. (1998) Time constraints on the Early Paleozoic docking of the Precordillera, central Argentina. In: Pankhurst, R.J. and Rapela, C.W. (Eds.), *The Proto-Andean margin of Gondwana*. Geol. Soc. Lon. Spec. Pub., v. 142, pp. 143-158.
- Rapela, C.W. and Pankhurst, R.J. (2002) Eventos tectomagmáticos del Paleozoico Inferior en el margen protoatlántico del sur de Sudamérica. 15° Cong. Geol. Argentino, Actas, 1, pp. 24-29.
- Rapela, C.W., Pankhurst, R.J., Casquet, C., Baldo, E., Saavedra, J., Galindo, C. and Fanning, C.M. (1998) The Pampean Orogeny of the southern proto-Andes: Cambrian continental collision in the Sierras de Córdoba. In: Pankhurst, R.J. and Rapela, C.W. (Eds.), *The Proto-Andean margin of Gondwana*. Geol. Soc. Lon. Spec. Pub., v. 142, pp. 181-217.
- Sato, A.M., Tickyj, H., Llambías, E.J. and Sato, K. (2000) The Las Matras tonalitic-trondhjemitic pluton, central Argentina: Grenvillian-age constraints, geochemical characteristics, and regional implications. *J. S. Amer. Earth Sci.*, v. 13, pp. 587-610.
- Sato, A.M., González, P.D. and Llambías, E.J. (2003) Evolución del orógeno Famatiniano en la Sierra de San Luis: magmatismo de arco, deformación y metamorfismo de bajo a alto grado. *Rev. Asoc. Geol. Argentina*, v. 58, pp. 487-504.
- Sato, K. and Kawashita, K. (2002) Espectrometría de masas em Geología Isotópica. *Rev. Inst. Geociências-USP, Geol. USP Ser. Cient.*, São Paulo, v. 2, pp. 57-77.
- Simpson, C., Law, R.D., Gromet, L.P., Miró, R. and Northrup, C.J. (2003) Paleozoic deformation in the Sierras de Córdoba and Sierra de las Minas, eastern Sierras Pampeanas, Argentina. *J. S. Amer. Earth Sci.*, v. 15, pp. 749-764.
- Steiger, R.H. and Jäger, E. (1977) Convention on the use of decay constants in geo and cosmochronology. *Earth Planet. Sci. Lett.*, v. 36, pp. 359-362.
- Tickyj, H. (1999) Estructura y petrología del Basamento Cristalino en la región centro-sur de la provincia de La Pampa, Argentina. Univ. Nac. La Plata (Argentina), Unpub. Doctoral Thesis. 229p.
- Tickyj, H., Basei, M.A.S., Sato, A.M. and Llambías, E.J. (1999) U-Pb and K-Ar ages of Pichi Mahuida Group, crystalline basement of SE La Pampa province, Argentina. 2° S. Amer. Symp. Isotope Geol., Ext. abst., pp. 139-142.
- Tickyj, H., Llambías, E.J. and Melchor, R.N. (2002) Ordovician rocks from La Pampa province, Argentina. In: Aceñolaza, F.G. (Ed.), *Aspects on the Ordovician system of Argentina*. Univ. Nac. Tucumán, INSUGEO, Serie Correlación Geológica, v. 16, pp. 257-266.
- Varela, R. and Dalla Salda, L.H. (1992) Geocronología Rb-Sr de metamorfitas y granitoides del terciario sur de la Sierra de Pie de Palo, San Juan, Argentina. *Rev. Asoc. Geol. Argentina*, v. 47, pp. 271-275.
- Varela, R., Cingolani, C., Sato, A.M., Dalla Salda, L., Brito Neves, B.B., Basei, M.A.S., Siga Jr, O. and Teixeira, W. (1997) Proterozoic and Paleozoic evolution of Atlantic area of North-Patagonian Massif, Argentina. 1st S. Amer. Symp. Isotope Geol., Actas, pp. 326-329.
- Varela, R., Basei, M.A.S., Sato, A.M., Siga Jr, O., Cingolani, C. and Sato, K. (1998) Edades isotópicas Rb/Sr y U/Pb en rocas de Mina Gonzalito y Arroyo Salado, Macizo Norpatagónico Atlántico, Río Negro, Argentina. 10° Cong. Latinoamer. Geología, Actas, 1, pp. 71-76.
- Varela, R., Basei, M.A.S., Sato, A.M., González, P.D., Siga Jr, O., Campos Neto, M. Da C. and Cingolani, C.A. (2003a) Grenvillian basement and Famatinian events of the Sierra de Umango (29°S): a review and new geochronological data. 4° S. Amer. Symp. Isotope Geol., pp. 304-306.
- Varela, R., Sato, A.M., Basei, M.A.S. and Siga Jr, O. (2003b) Proterozoico Medio y Paleozoico Inferior de la Sierra de Umango, Antepaís Andino (29°S), Argentina. Edades U/Pb y caracterizaciones isotópicas. *Rev. Geol. Chile*, v. 30, pp. 265-284.
- Vujovich, G.I., Van staal, C.R. and Davis, W. (2004) Age constraints on the tectonic evolution and provenance of the Pie de Palo complex, Cuyania composite terrane, and the Famatinian Orogeny in the Sierra de Pie de Palo, San Juan, Argentina. *Gondwana Res.*, v. 7, pp. 1041-1056.